



Published in final edited form as:

Differentiation. 2019 ; 105: 54–70. doi:10.1016/j.diff.2019.01.005.

Hepatic differentiation of human pluripotent stem cells by developmental stage-related metabolomics products

Sriram Bandi^{1,2,1}, Tatyana Tchaikovskaya^{1,2}, and Sanjeev Gupta^{1,2,3,4,5,6,*}

¹Department of Medicine, Albert Einstein College of Medicine, Bronx, NY 10461, USA

²Marion Bessin Liver Research Center, Albert Einstein College of Medicine, Bronx, NY 10461, USA

³Department of Pathology, Albert Einstein College of Medicine, Bronx, NY 10461, USA

⁴Diabetes Center, Albert Einstein College of Medicine, Bronx, NY 10461, USA

⁵Irwin S. and Sylvia Chanin Institute for Cancer Research, Albert Einstein College of Medicine, Bronx, NY 10461, USA

⁶Ruth L. and David S. Gottesman Institute for Stem Cell and Regenerative Medicine Research, Albert Einstein College of Medicine, Bronx, NY 10461, USA

Abstract

Endogenous cell signals regulate tissue homeostasis and are significant for directing the fate of stem cells. During liver development, cytokines released from various cell types are critical for stem/progenitor cell differentiation and lineage expansions. To determine mechanisms in these stage-specific lineage interactions, we modeled potential effects of soluble signals derived from immortalized human fetal liver parenchymal cells on stem cells, including embryonic and induced pluripotent stem cells. For identifying lineage conversion and maturation, we utilized conventional assays of cell morphology, gene expression analysis and lineage markers. Molecular pathway analysis used functional genomics approaches. Metabolic properties were analyzed to determine the extent of hepatic differentiation. Cell transplantation studies were performed in mice with drug-induced acute liver failure to elicit benefits in hepatic support and tissue regeneration. These studies showed signals emanating from fetal liver cells induced hepatic differentiation in stem cells. Gene expression profiling and comparison of regulatory networks in immature and mature

* **Correspondence:** Sanjeev Gupta, MD, Albert Einstein College of Medicine, Ullmann Building, Room 625, 1300 Morris Park Avenue, Bronx, NY 10461; Tel: 718 430 3309; Fax: 718 430 8975.

Author contributions

SB performed experiments, acquired and interpreted data; TT analyzed data and interpreted results. Corresponding author designed study, obtained funding, analyzed and interpreted data. All authors contributed to preparing and approving the final manuscript.

¹**Present address:** SB: Technical Operations, Cell Therapy Process Development, Sangamo Therapeutics, 501 Canal Boulevard, Richmond, CA 94804

Publisher's Disclaimer: This is a PDF file of an unedited manuscript that has been accepted for publication. As a service to our customers we are providing this early version of the manuscript. The manuscript will undergo copyediting, typesetting, and review of the resulting proof before it is published in its final citable form. Please note that during the production process errors may be discovered which could affect the content, and all legal disclaimers that apply to the journal pertain.

Conflict of interest statement:

Albert Einstein College of Medicine filed for intellectual protection with certain rights to SB and SG. TT declares no competing interests exist.

hepatocytes revealed stem cell-derived hepatocytes represented early fetal-like stage. Unexpectedly, differentiation-inducing soluble signals constituted metabolomics products and not proteins. In stem cells exposed to signals from fetal cells, mechanistic gene networks of upstream regulators decreased pluripotency, while simultaneously inducing mesenchymal and epithelial properties. The extent of metabolic and synthetic functions in stem cell-derived hepatocytes was sufficient for providing hepatic support along with promotion of tissue repair to rescue mice in acute liver failure. During this rescue, paracrine factors from transplanted cells contributed in stimulating liver regeneration. We concluded that hepatic differentiation of pluripotent stem cells with metabolomics products will be significant for developing therapies. The differentiation mechanisms involving metabolomics products could have an impact on advancing recruitment of stem/progenitor cells during tissue homeostasis.

Graphical Abstract

fx1

Keywords

Cell therapy; endoderm; gene expression; liver; transcription; regenerative medicine

INTRODUCTION

Hepatic differentiation of human pluripotent stem cells (PSC), i.e., embryonic stem cells (hESC) or induced pluripotent stem cells (hiPSC), is needed for disease models, translational applications and cell therapy. Protocols that allow stem cell differentiation in rapid, efficient and inexpensive ways will advance these areas, but defining suitable signals and cues requires more progress. Previously, lineages from PSC were generated through embryoid bodies [1], incorporation of chemicals and cytokines (dexamethasone, activin A, retinoic acid, HGF, oncostatin M, others) [2–7], some of which might have contributed cytoprotective or growth-inducing properties. or co-culture with nonparenchymal liver cell types (endothelial, stellate cell or cholangiocyte cell lines) [8], but inductive signals directing differentiation remained unknown. Separating differentiated cells from complex mixtures was especially important because mixed cell populations incorporating undifferentiated or less differentiated cell types may result in tumorigenesis [9]. Subsequently, adoption of step-wise signals deduced from hepatic ontology helped in guiding differentiation of PSC [10–13]. Also, nuclear reprogramming by transcription factors (TFs) was helpful: For instance, pancreatic beta cells were generated from fetal hepatoblasts (by expressing the homeobox gene, PDX1) [14]; or hepatocytes from fibroblasts (by combined expression of TFs - FOXA3, HNF1 α and HNF4 α ; or HNF1 α , HNF4 α , HNF6, ATF5, PROX1, and CEBPa) [15, 16]. More recent studies emphasized that step-wise switches to coordinate multiple intracellular pathways improved hepatic differentiation [17].

Cell transplantation studies in mouse models have been appropriate for verifying metabolic properties in stem cell-derived cells, e.g., through amelioration of diabetes (beta cells) or detoxification functions (hepatocytes) [14, 16]. However, proliferation in mice of human cells, including stem cell-derived hepatocytes is generally restricted. This has required

addition of oncogenes, such as SV40 T antigen in transplantation studies [16, 17]. On the other hand, transgene integrants, including constructs of TFs, may be deleterious due to insertional mutagenesis. Therefore, alternative approaches are of major interest for nuclear reprogramming, e.g., small molecules. Chemicals have been successfully used in conjunction with HNF α for reprogramming fibroblasts from mesenchymal to epithelial fate [18]. Remarkably, in mouse ESC exposure to metabolomics or other small molecules led to either maintenance of pluripotency or increased differentiation (cardiac or neuronal) [19, 20]. These molecules were proposed to have altered intracellular redox states and inflammation. Whereas, efforts to achieve directed differentiation of PSC for hepatic or biliary fates provided advances [21–23], differentiation to adult stages remains elusive. Typically, identification of differentiation stages in PSC has been infirm without delineation for this purpose of molecular “gold standards”.

During ontogeny in human liver, fetal hepatocytes (FH) display multi-lineage markers (mesenchymal, epithelial, hepatobiliary) along with stem-like potential [24–26]. Cells resembling FH are sequestered within ductal niches of the adult liver [26], where these may be recruited during disease states for replacement of hepatocytes [27]. As lineage transitions during embryonic - fetal - adult stages offer frameworks for characterizing PSC differentiation, this was tested in hESC-derived cells displaying hepatic meso-endodermal phenotype with coexpression of epithelial and mesenchymal genes, compared with FH or adult hepatocytes (AH) [28]. Modeling of mechanistic molecular networks based on transcriptomic analyses indicated FH and AH rapidly regressed in culture. Hepatic differentiation was particularly restricted by the extinction of regulatory TFs (HNF4 α , HNF1, others), which likely concerned promoter methylation [29]. Post-transcriptional mechanisms also involve microRNAs (miRNA), which are significant for cell maintenance, but did not direct stem cell differentiation [28]. Modeling of such stage-specific transcriptional context will be important for identifying cell differentiation states; and then for overcoming specific restriction points.

As interactions with other cell types may alter fate of PSC, e.g., RBCs were produced by interactions of hESC with cells from fetal liver (site for extramedullary hematopoiesis offers physiological connection) [30], we considered that hepatic differentiation may also be regulated by signals from FH. Here, we show that culture of hESC or hiPSC with conditioned medium (CM) from FH immortalized by human telomerase reverse transcriptase (hTERT), as previously characterized [14, 31], generated hepatocytes. Differentiation staging by molecular network analysis compared with natural hepatocytes allowed characterization of their lineage state. This indicated that PSC-derived hepatocytes were early fetal hepatocyte-like cells – leading us to designate these as “eFHLC”. The nature of signals in hTERT-FH-CM driving this stem cell differentiation was unexpected - these were revealed as small metabolomics products and not proteins. The repertoire of hepatic properties in PSC-derived hepatocytes suggested therapeutic potential, which was elicited by cell transplantation studies in mice with induced acute liver failure (ALF). Hepatocytes derived from PSC by hTERT-FH-CM rescued these animals through a combination of metabolic support and stimulation of liver regeneration by paracrine factors otherwise deficient in ALF. The molecular pathways in stem/progenitor cells for endogenous

metabolomic products should be relevant too under noninjury conditions for tissue homeostasis.

MATERIALS AND METHODS

Approvals.

The IRB, Embryonic Stem Cell Research Oversight Committee, and Animal Care and Use Committee at Einstein approved studies according to local and federal regulations. Fetal tissues of 18-20 weeks were from Einstein Human Fetal Tissue Repository or Advanced Bioscience Resources (Alameda, CA).

Reagents, chemicals and drugs.

Unless specified, these were from Sigma-Aldrich (St. Louis, MO). Metabolomic chemical products (CP) were purchased (Sigma-Aldrich or Santa Cruz Biotechnology, Santa Cruz, CA). Stocks of CP were in water or ethanol according to recommendations from manufacturers.

Liver cells.

Mid-gestation primary fetal hepatocytes (FH) were isolated by Ep-CAM+ immunomagnetic sorting as previously described [24, 26]. For CM, we used hTERT-FH-B cells previously derived from mid-gestation fetal livers and that retain properties of FH [31]. These cells were cultured for 24h in DMEM/F12 medium with 2% Knock-out Serum Replacer (KSR), 2 mM L-glutamine, 0.1 mM MEM, NEAA, 1% penicillin-streptomycin (Invitrogen Corp., Carlsbad, CA). HepG2 cells were originally from American Type Culture Collection (ATCC, Manassas, VA). These were authenticated by genotyping. Cell culture used RPMI1640 medium with 10% fetal bovine serum and antibiotics.

hESC/hiPSC.

WA-01 hESC were from WiCell (Wisconsin, MD). Healthy human fibroblasts were used in Einstein's Pluripotent Stem Cell Core to generate hiPSC by CytoTune-iPS Sendai Reprogramming Kit (Cat#A1378001; Life Technologies, Carlsbad, CA). Cells were maintained in culture on matrigel in DMEM/F12 medium with 1% B27 and 1% N2 supplements, 2 mM L-glutamine, 0.1 mM non-essential amino acids (NEAA) (Invitrogen Corp., Carlsbad, CA) and 50 ng/ml bFGF (R&D Systems, Minneapolis, MN).

In some studies, cell culture with hTERT-FH-CM included additives as follows: 2 μ M retinoic acid (RA) (Sigma) from d0-d3; 20 ng HGF (PeproTech Inc., Rocky Hill, NJ), 10^{-8} nmol dexamethasone, 1% B27 supplement from d3-d6; 20 ng/ml hepatocyte growth factor (HGF) and oncostatin M (OSM) (R&D Systems), 10^{-8} nmol dexamethasone, 1% B27 supplement from d7-d14; in part based on prior protocols (GFs and additives) [2-7]. Dexamethasone was aimed at depleting fibroblast-like cells; HGF and OSM were included largely for their cytoprotective effects, as previously found for cultured FH [25]. The differentiation effect of GFs and additives with or without hTERT-FH-CM was studied in hESC. These cells were plated in hTERT-FH-CM (or its protein and chemical components).

In some studies, GFs and additives were included on days indicated above after hESC had attached in dishes.

Cytotoxicity assays.

Primary mouse hepatocytes were isolated by collagenase perfusion [32]. Cells were plated overnight in 48-well dishes (1.5×10^5 per well) in RPMI 1640 medium with 10% FBS. These were incubated with actinomycin D and then 10 ng/ml TNF- α (Sigma) with or without CM for MTT assays after another 16–18h [33].

EM.

Cells were fixed in 2.5% glutaraldehyde in cacodylate buffer, postfixed in osmium tetroxide, and stained with 1% uranyl acetate before embedding in plastic.

Cytokine arrays.

Human antibody Array I (507 proteins, AAH-BLM-1-2) and Human RTK Phosphorylation Antibody Array 1 (71 proteins, AAH-PRTK-1-2) (RayBiotech, Norcross, GA) were used according to manufacturer.

Metabolic functions.

Medium harvested after 3h was analyzed for human albumin with immunoassay (Bethyl Laboratories, Montgomery, TX). For ureagenesis, cells were incubated with 2.5–7.5 mM ammonium chloride for 12h and analyzed as described [34]. For CYP450, 7-ethoxyresorufin conversion was analyzed as described [35].

Molecular studies.

RNA was extracted by TRIzol reagent (Invitrogen), cleaned by RNeasy (Qiagen Sciences, Germantown, MD), incubated in DNase I (Invitrogen) and reverse-transcribed by Omniscript RT kit (Qiagen). Platinum PCR SuperMix (Invitrogen) was used with annealing at $94^{\circ}\text{C} \times 5$ min, and 35 cycles at $94^{\circ}\text{C} \times 30\text{s}$, $55^{\circ}\text{C} \times 30\text{s}$, $72^{\circ}\text{C} \times 45\text{s}$, and $72^{\circ}\text{C} \times 10$ min (**primers in** Suppl. Table S1). Mouse Stress and Toxicity RT² Profiler PCR Array (PAMM-003A) and RT² Real-Time SyBR Green PCR mix and RT² First Strand kit were from SA Biosciences (Frederick, MD). Quantitative (q) RT-PCR used customized arrays for 24 pluripotency, TFs or hepatobiliary genes (CAPH-0800A; SA Biosciences). Data were analyzed by 2^{-Ct} method. Expression difference of 2-fold up or down was considered significant. Gene expression analysis with U133 2.0 Plus arrays (Affymetrix Corp., Santa Clara, CA) used Affymetrix Transcription Analysis Console, version 4 (TAC) as described [25, 28]. Differences of 5-fold were annotated. Pathways were examined by IPA tools (Ingenuity Systems Inc., Redwood, CA) [28]. Gene expression datasets are in NCBI's Gene Expression Omnibus [36], with access through GEO Series accession numbers GSE108047, GSE108048 and GSE115410 (<https://www.ncbi.nlm.nih.gov/geo/query/acc.cgi?acc=GSExxx>).

Immunostaining.

Cells were fixed in 4% paraformaldehyde in phosphate buffered saline, pH 7.4 (PBS), blocked/permeabilized with 5% goat serum, 0.2% Triton X-100 (Sigma) in PBS for 1h, and incubated overnight at 4°C with antibodies for human OCT3/4 (1:200), α -fetoprotein (AFP) (1:100), E-cadherin (ECAD) (1:50) (Santa Cruz), FOXA2 (1:100) (R&D Systems), albumin (ALB) (1:200) (Sigma), or vimentin (VIM) (1:100) (US Biologicals, Swampscott, MA). After washing in PBS, TRITC-conjugated goat anti-mouse IgG (1:50, Sigma) or anti-rabbit IgG (1:100) were added for 1h with 4'-6-diamidino-2-phenylindole (DAPI) (Invitrogen) counterstaining. Primary antibodies were omitted in negative controls. Glycogen, glucose-6-phosphatase (G-6-P), and γ -glutamyl transpeptidase (GGT) were stained as previously described [26, 37].

Tissue studies.

Cryostat sections were used for H&E staining. Tissue injury was graded as previously described [32]. For hepatic functions, glycogen and G-6-P were stained [34]. For Ki67 and histone γ H2AX, tissues were fixed in 4% paraformaldehyde in PBS. Rabbit anti-Ki67 (1:750, Vector Labs., Burlingame, CA) or rabbit anti- γ H2AX (1:300, ab2893; Abcam, Cambridge, MA), were applied followed by secondary anti-rabbit Alexa Fluor 546 (1:500, Molecular Probes), and DAPI counterstaining [32, 37]. Transplanted cells were identified by in situ hybridization with digoxigenin-labeled centromeric probe for primate alphoid satellite sequences as previously described [38].

Mouse model of ALF.

CB17.NOD/SCID^{prkdc} mice, 6-7 weeks old, were from Jackson Labs. (Bar Harbor, ME). For ALF, mice were given i.p. rifampicin - Rif (75 mg/kg) and phenytoin - Phen (30 mg/kg) daily for 3d and i.p., monocrotaline - MCT (160 mg/kg) on day 4 as previously described [32]. After 1d, $4-6 \times 10^6$ hESC-derived cells were transplanted i.p. with 1 ml Cytodex 3TM microcarriers (Sigma). Mice were observed for 2 weeks. Encephalopathy was graded from 0 (absent) to 3 (coma).

Statistical methods.

Data are shown as means \pm SEM. Significance was analyzed by t-tests, Chi-square, or analysis of variance (ANOVA). IPA used built-in statistical tools. A web enabled tool was used for depicting heat maps and pairwise comparisons [39]. Statistical analysis used GraphPad Prism7 (GraphPad, San Diego, CA). Charts were prepared with SigmaPlot 9.0 (Systat Software Inc. San Jose, CA). $P < 0.05$ was considered significant.

RESULTS

Exposure to hTERT-FH-CM induced hepatic differentiation in hESC

Undifferentiated hESC displayed characteristic morphology with discrete colonies of small cells containing scanty cytoplasm that were tightly arranged next to one another (Fig. 1A). In the presence of medium containing GFs and additives alone, hESC morphology was variably altered with intermingled areas still containing undifferentiated hESC. On the other

hand, after 3d in GFs and additives plus hTERT-FH-CM, hESC uniformly assumed epithelial morphology. This difference was pronounced over time, such that after 13-14d, hESC-derived eFHLC developed larger nuclei with greater cytoplasmic abundance and complexity. Binucleated cells constituted another hepatic characteristic. This eFHLC morphology compared favorably with freshly-isolated primary FH, including similar hepatocyte-like nuclei and organelles, e.g., micro-peroxisomes (Fig. 1B). Typically, $0.50 \pm 0.07 \times 10^6$ hESC produced $1.94 \pm 0.05 \times 10^6$ eFHLC over 14d (4-fold expansion). From primary culture (P0) to second passage (P2), eFHLC numbers increased >20-fold.

Culture of hESC in hTERT-FH-CM alone yielded uniform populations of epithelial cells within 3d that were similar to those after GFs and additives plus hTERT-FH-CM. However, these cells survived and proliferated inefficiently beyond 3-4d. As the condition of GFs and additives incorporated RA (0-3d) plus HGF and OSM (3-6d) during this period, these were then included for further analysis.

For effects in hESC of GFs and additives with or without hTERT-FH-CM, we examined by qRT-PCR expression of representative genes ($n=23$) (Suppl. Table S2). After hESC culture in basal medium plus GFs and additives alone for either 3d or 13d, pluripotency markers (OCT4, NANOG and SOX2) were not extinguished and gain of endoderm and mesoderm markers was limited. By contrast, in hESC cultured with GFs and additives plus hTERT-FH-CM, gene expression in resultant eFHLC was markedly different with loss of pluripotency markers (OCT4, NANOG, SOX2); and transient gain of endoderm (SOX17, FOXA2) or mesoderm (brachyury) markers. This was followed after 14d by greater expression of hepatic TFs (GATA4, HNF1A, HNF4A), simultaneous epithelial (E-CAD), mesenchymal (VIM) and biliary (CK-19) properties, switching of AFP and ALB expression characteristic of fetal-neonatal transition, and other hepatic genes (α -1 antitrypsin – AAT; transthyretin – TTR; cytochrome P450s - CYP3A4 or CYP7A1). Pairwise gene expression comparisons for GFs and additives with or without hTERT-FH-CM indicated differences were significant, $p < 0.0006$, ANOVA (Fig. 2A). After 14d, mRNA levels in hESC cultured with GFs and additives alone or plus hTERT-FH-CM were mean of 2.0 ± 0.3 -fold versus 82 ± 35 -fold above untreated controls, respectively, $p < 0.001$. This indicated GFs and additives contributed minimally or very little to hepatic differentiation. Therefore, for further analysis, we considered that including GFs and additives alone as a separate control was not worthwhile.

For developmental staging, mRNA expression in hESC, FH and AH was modeled. Clustering of mRNA profiles indicated eFHLC and undifferentiated hESC diverged within 3d (Fig. 2B). After 13d, eFHLC clustered along FH undergoing three passages in culture (FH-P3)). Previously, mRNA and miRNA profiles in such FH-P3 had established differentiation regression versus freshly-isolated FH (PP), leading to phenotype-sharing with hESC-derived meso-endodermal cells [28]. Analysis of gene ontology differences indicated eFHLC differed substantially from hESC (Fig. 2C). Within 3d of differentiation in eFHLC, the ontology pathways assuming topmost significance concerned sternness: hESC pluripotency; hepatic fibrosis/hepatic stellate cell activation; and role of NANOG in mammalian ESC pluripotency (Suppl. Table S3 – **Excel**). After 13d, sternness groups decreased, and significance of hESC pluripotency or NANOG pathways was supplanted by hepatic fibrosis/hepatic stellate cell activation (Suppl. Table S4 – **Excel**). This inflammatory

change was reminiscent of stress or related alterations in cellular and molecular functions in hESC-derived meso-endodermal cells [28]. Co-expression of mesenchymal and epithelial genes in freshly-isolated or cultured primary FH was previously characterized [25].

Molecular pathways in hepatic differentiation of eFHLC

To determine the nature of reprogramming, we examined upstream transcriptional regulators (TRs). Within 3d of eFHLC generation by GFs and additives with hTERT-FH-CM substantial differences were apparent in TRs (n=36; >5-fold up or down in eFHLC versus hESC with prioritization for p values of nonoverlap) (Suppl. Table S5). During continued differentiation over 13d, more TRs were recruited (n=75). This concerned downregulation of pluripotency drivers (OCT4, NANOG or SOX2); and upregulation of differentiation regulators (WNT, frizzled, β -catenin, GATA6 and others). These differences were well-illustrated by mechanistic networks for NANOG (inactivated) or GATA6 (activated) (Fig. 3). Inflammation-related events were also prominent, i.e., cytokines (TNF, IL1, TGF β), prostanoid (PGE2), intracellular mediators (NF-kB, RELA), and others.

To dissect potential contributions of RA, HGF and OSM in differentiation versus cytoprotective or anti-inflammatory processes, we examined eFHLC derived from hESC by GFs and these additives plus hTERT-FH-CM. In eFHLC after 3d with exposure to hTERT-FH-CM plus only RA, expression of HGF, OSM and its receptor, OSMR, was absent although MET (HGF receptor) was induced (6-fold above hESC). Of retinoic acid receptors, RARA and RARB were expressed (8-fold and 7-fold above hESC, respectively), but RXRA was not expressed. With further differentiation over 13d of eFHLC in presence of hTERT-FH-CM plus GFs and additives, OSMR was expressed (40-fold above hESC). expression of MET and RARA continued (10-fold and 5-fold above hESC, respectively), although HGF, OSM, RARB and RXRA were not expressed. The downstream TR networks of HGF, OSM, RARA and RARB did not assume significant p values of nonoverlap (Suppl Table S5). Nonetheless, delineation of these HGF and OSM networks revealed representation largely of cytoprotective and inflammation- or cell growth-related processes (Fig. 4). Similarly, the effects of RAR and RXRA networks suggested regulation of multiple pathways besides those contributing in differentiation (Suppl Fig. S1). This was in agreement with little effects on hepatic differentiation of GFs and other additives in the absence of hTERT-FH-CM. On the other hand, GFs did contribute in survival and growth of eFHLC.

The extent of hepatic differentiation by mRNA expression in eFHLC was inferior to freshly-isolated FH-PP or AH; it equilibrated more with FH-P3. Both in eFHLC and FH-P3, the three topmost canonical pathways differing from FH-PP were identical: FXR/RXR activation; LXR/RXR activation; and acute phase response signaling. This re-emphasized roles of nuclear signaling and inflammation.

Upstream regulators informed on mechanistic role of endogenous signals. Compared with FH-PP, the activation and inactivation patterns of mechanistic TR networks were shared in eFHLC (n=87) and FH-P3 (n=62) (see Suppl. Tables S6). Less active TR networks in eFHLC and FH-P3 included those of CEBPA; whereas more active TR networks included that of SNAI2 (Fig. 5). This was in agreement with meso-endodermal phenotype in eFHLC

or FH-P3 vs FH-PP, since CEBP and related TRs regulate hepatic genes; whereas SNAI and related members regulate mesenchymal genes.

Metabolic and other hepatic functions were expressed in differentiated cells

Results from pathway analysis were confirmed at protein and biochemical levels. Studies in eFHLC generated by hTERT-FH-CM plus GFs and additives from either hESC or hiPSC verified declines in stem cell markers (OCT4, NANOG, TRA-1-80) (from 100% to 0% cells), $p < 0.001$ (Fig. 6A-B). These markers were also absent in control FH. Plasma membrane localization of ECAD in eFHLC was similar to control FH. Presence of this marker in 100% of eFHLC indicated epithelial conversion was highly efficient. This was consistent with β -catenin-related events identified by mRNA expression analysis. Co-expression of VIM (mesenchymal marker) in 100% of eFHLC, as well as control FH, verified meso-endodermal phenotype. This was also in agreement with mRNA expression of TRs. In eFHLC, hepatic markers were gained (FOXA2, ALB, G6P, glycogen in up to 100% though with cell-to-cell expression differences). AFP was sparsely expressed. Biliary markers (GGT, CK-19) were present in 100% cells (Fig. 6B). This was similar to FH. Significant fractions of eFHLC (~30%) expressed asialoglycoprotein receptor (ASGPR1) (Fig. 6C). In case of FH-PP 60-70% cells expressed ASGPR1, $p < 0.001$, indicating eFHLC were less mature. This was in agreement with lower hepatic TR activity in the latter.

Hepatic differentiation by CM from hTERT-FH involved metabolomics products

To identify constituents of FH-CM imparting differentiation, we used protein arrays and these revealed expression of 62 cytokines and growth factors (from total $n=507$) (Suppl. Fig. S2). For effects in cells, these ligands should have engaged receptors-this was examined by exposing hESC to FH-CM (10 min, 1h and 6h), and probing of numerous receptor tyrosine kinases (RTKs) ($n=71$). Ligands were identified in FH-CM for at least 12 RTKs (activinA, FGFs, TGF, others) (Suppl. Fig. S3). However, no RTK was activated in hESC that had been exposed to FH-CM.

To determine the requirement of proteins in FH-CM for PSC differentiation, these were degraded by heating (to 100°C) and size exclusion (>3 kilodalton proteins) by Amicon membranes. Despite protein degradation or depletion, FH-CM still advanced differentiation in hESC within 3d, just as before. Epithelial morphology was induced, expression of pluripotency genes declined (NANOG, SOX-2), and that of epithelial (AFP), or mesenchymal (VIM) genes increased (Suppl. Fig. S4). Thus, we surmised that alternative nonprotein components were contributing in cell differentiation. These were apparently heat-stable (to 100°C), and also long-lived, since eFHLC were generated despite storage of FH-CM for 6 weeks at 4°C (not shown).

We characterized metabolomics products in FH-CM by LC-MS in the Metabolite Profiling Facility at Purdue University. Good separations were reported in blank medium and FH-CM for 810 classes; of these, 105 classes were 3-fold abundant, $p < 0.03$ (Suppl. Table S7). Then cell differentiation was tested with eight off-the-shelf chemical products (CPs) (Suppl. Table S8). In these studies, CPs were added followed by GFs and additives to reproduce hTERT-FH-CM conditions. Individually, none of the CPs differentiated hESC - cell morphology was

unchanged; OCT4 was expressed and ALB or VIM were absent. However, combining 7 or 8 CPs together generated eFHLC with loss of OCT4 (in 100%) and gain of ALB and VIM (in 50--90%) (Fig. 7A). Metabolic functions were also recapitulated with urea synthesis and xenobiotic conversion (Fig. 7B). This was similar to eFHLC generated by hTERT-FH-CM. Moreover, CPs induced loss of pluripotency markers in hiPSC, along with hepatic differentiation to fetal-like stage (Suppl. Fig. S5).

Transplantation of eFHLC was sufficient for rescue in ALF

Multiple types of liver injuries, including drug toxicity and viral hepatitis, may cause ALF [40]. In this situation, deficiency of VEGF, PDGF and other cytokines or chemokines increases susceptibility to sepsis, impaired liver regeneration and mortality [41, 42]. Excess of proliferation-inhibiting cytokines, such as TGF- β , also impairs liver regeneration [43]. By contrast, replacement in ALF of deficient metabolic functions and paracrine factors through ectopic hepatic transplantation allows liver regeneration [32, 37, 44]. Therefore, we studied whether eFHLC would provide suitable metabolic functions and cytokines for rescue in ALF. Protein arrays for cytokines demonstrated VEGF, PDGF and GCSF were secreted by eFHLC (Suppl. Fig. S6). Testing of CM from eFHLC showed this protected primary mouse hepatocytes from TNF- α cytotoxicity (Fig. 8A). Quantitation of hepatic functions in eFHLC revealed albumin or urea synthesis and xenobiotic conversion (ethoxyresorufin to resorufin) (Fig. 8B). These functions were less than in HepG2 cells, $p < 0.05$ [45]. As viability and function of primary human hepatocytes is highly variable depending on donor liver quality, HepG2 cells are commonly used for this purpose [17]. Moreover, mapping of upstream regulators in eFHLC indicated HNF4A and HNF1B mRNA networks were active (Fig. 8C-D), which was in agreement with these metabolic functions.

To determine whether eFHLC would support liver regeneration, we studied NOD/SCID mice with drug-induced ALF ($m=20$) [32, 37]. Mice received i.p scaffolds with $4-6 \times 10^6$ eFHLC ($n=10$), and controls, scaffolds alone ($n=10$). In eFHLC recipients, 5 mice (50%) survived; only 1 control mouse (10%) survived, $p < 0.001$ (Fig. 9A). Encephalopathy decreased after eFHLC, versus controls, $p < 0.05$. Liver tests also improved; after 7d, serum alanine aminotransferase (ALT), 77 ± 82 vs 4800 ± 500 u/l, $p < 0.001$; total serum bilirubin, 0.5 ± 0.2 vs 2.5 ± 0.5 mg/dl; $p < 0.05$; blood glucose and creatinine levels were normal. Human-specific molecular probe identified eFHLC transplanted into the peritoneal cavity were engrafted (Fig. 9B). The liver of control mice had significant necrosis. Extensive γ H2AX expression indicated hepatic DNA damage. As Ki-67+ cells were infrequent, this indicated absence of liver regeneration (Fig. 9C). By contrast, after eFHLC transplantation, liver necrosis, as well as γ H2AX expression decreased; and prevalence of Ki-67+ cells increased (Fig. 9D). Tissue grading showed 5.4-fold less injury after 7d, 0.7 ± 0.3 vs 3.8 ± 0.4 , $p < 0.05$ (Fig. 9E). Ki-67+ cells were 2.3-fold more prevalent, 91 ± 5 vs 39 ± 4 cells/HPF, $p < 0.05$ (Fig. 9F).

Liver gene expression was altered in ALF, including pathways of oxidative/metabolic stress, inflammation, DNA damage and cell cycling. These abnormalities improved 3d-7d after eFHLC transplants (Suppl. Table S9). Therefore, metabolic support and paracrine signals from eFHLC advanced liver regeneration in ALF.

DISCUSSION

The ability of metabolomics molecules to induce stage-specific differentiation of PSC rapidly and efficiently will be significant. We obtained firm evidence for hepatic differentiation in PSC with metabolomics candidates. These induced differentiation in concert with other additives, including GFs and retinoic acid that by themselves exerted only limited effects. Previously, loss-of function through antagonism in hESC-MEC or FH-P3 of WNT, NOTCH or histone deacetylation mechanisms by DKK-1, γ -secretase inhibitor X or trichostatin, respectively, was unrewarding for hepatic differentiation [46]. The loss-of-function from these molecules was not further helpful for differentiation of hESC with hTERT-FH-CM (not shown). Comprehensive investigation of each metabolomics class represented in hTERT-FH-CM was beyond the scope of our studies.

The underlying mechanisms in differentiation by metabolomics products concerned broad effects on transcription regulation and additional processes. Mechanistically, endogenous metabolites were able to promote either pluripotency or cardiac and neuronal differentiation by altering cellular redox activities or inflammation [19]. Suppression of these processes preserved pluripotency; their activation resulted in cell differentiation. In our studies, differentiation-inducing CPs included major regulators of redox states. As maintenance of cellular redox incorporates disulfide-thiol exchanges [47], glutathione (and possibly D-penicillamine) disulfides may have contributed to PSC differentiation in this way. Glutathiones are important for hepatic injury and inflammation: Excessive anti-oxidant depletion causes mitochondrial damage and cell-growth arrest in ALF [48]; glutathione replacement by N-acetyl cysteine (NAC) benefits recovery in ALF [41]. Tissue regeneration by NAC (in retina) involved stem/progenitor cell renewal [49]. This was independent of growth factor signaling (FGF) but included MAPK-1 or-3 pathways. Multiple intracellular signaling pathways were activated by hTERT-FH-CM during PSC differentiation. In this respect, glutathione activates cell survival and differentiation events via NF- κ B, WNT or NOTCH pathways (as in myogenic differentiation of mouse skeletal muscle cells or osteoblastic differentiation in human periodontal ligament cells) [50, 51].

Other CPs in hTERT-FH-CM likely contributed significantly in stem cell differentiation. For instance, the kynurenine pathway is significant for tryptophan degradation; it increases goblet cell differentiation in colonic cells [52]. Kynurenine advances osteoblast commitment in human mesenchymal stem cells in vitro and is required for osteogenesis in vivo [53]. Kynurenine also activates WNT, NOTCH and arylhydrocarbon receptor signaling in colon differentiation [52]. Among other CPs in hTERT-FH-CM, phytosphingosine has been associated with cardiac differentiation in mouse ESC and keratinocyte differentiation in skin [54, 55]; pyridoxine induces neuronal differentiation by upregulation of γ -aminobutyric acid-related systems in intact mice [56]; and phenacetin advances stem cell pluripotency through anti-inflammatory effects with inhibition of eicosanoid synthesis [19]. In combination, CPs probably exerted additional effects.

Specific mechanisms were activated in hESC by hTERT-FH-CM as indicated by activation and inactivation of TR networks. This was independent of GF-mediated signaling from RTKs, which suggested molecular events and processes were regulated biochemically.

Comparative gene expression identified intracellular effects of hTERT-FH-CM concerned many differentiation, inflammation and signaling pathways. Rapid entry of metabolomic products into cell compartments, including nucleus, should allow opportunities for modulation of reprogramming events. Differentiation in hESC cultured with hTERT-FH-CM was obvious within three days and gained further prominence thereafter, which was accompanied by recruitment of TRs. These alterations in differentiation were illustrated by coordinated regulation of NANOG and GATA6 networks. Numerous upstream TRs were regulated by soluble signals to indicate these exerted extremely broad effects on differentiation mechanisms. The effects of accompanying GFs and other additives in hTERT-FH-CM were largely related to cytoprotection and cell growth.

Staging of differentiation by gene expression profiling was helpful with application of effective comparators for characterizing eFHLC [28]. As early hepatic developmental stage includes coexpression of epithelial (ECAD, EpCAM, β -catenin), hepatic (AFP, ALB, G6P, glycogen), biliary (CK-19, GGT) and mesenchymal (VIM) properties in vivo [24, 26, 37], this was supported by similar phenotype in eFHLC. In cultured primary FH, hepatobiliary, epithelial and mesenchymal genes are similarly coexpressed [25]. Upstream TRs in eFHLC and cultured FH provided further mechanistic basis for this lineage stage. Hepatic differentiation was restricted by TRs (e.g., HNF4A, CEBPA), whereas mesenchymal differentiation was maintained by other TRs (e.g., TWIST1). Significantly, analysis of hESC-derived immature hepatocytes and FH or AH provided clues to major role for HNF4A [28]. Compared with primary FH or AH, HNF4A network was largely extinguished in hESC-derived hepatocytes. In cultured AH, HNF4A promoter is rapidly silenced by promoter methylation [29]. This was also the case in cultured FH (not shown). As downstream targets of HNF4A remain unmethylated, this accounts for the ability of autonomously driven transgenes for HNF4A or other TFs to force hepatic gene expression in nonpermissive cells [15, 16]. However, deleterious consequences from transgene shuffling or insertional mutagenesis makes alternative approaches necessary. Endogenous metabolomic products will cause no such concern.

Modeling development by molecular pathway regulation through functional genomics should be suitable for other lineages. As immaturity of stem cell-derived lineages is a universal problem, this will be particularly helpful for identifying restriction points in cell maturation. Generation by hTERT-FH-CM from PSC of foregut endoderm-like cells with endocrine properties will be relevant for additional lineages. In subsets of FH, PDX1 transgene induced insulin expression; this allowed correction of diabetes in mice [14]. Although metabolic functions may be tested in liver repopulation models, in a recent study, expansion after transplantation in liver of hepatocytes derived from fibroblasts with reprogramming from multiple TFs required immortalization with another SV40 oncogenic element [15].

Despite their immaturity, eFHLC rescued mice in ALF – where even small additions to liver function, along with complementation of deficient paracrine factors from healthy transplanted cells to promote liver regeneration, are of significance for survival [32, 37]. After intraperitoneal transplantation of hepatocytes in NOD/SCID mouse model of ALF used here, transplanted cells did not migrate to other organs (including liver, spleen and

lungs) [32]. Their benefits were thus related to extrahepatic metabolic support. Similarly, intraperitoneal transplantation of hESC-derived hepatocytes in meso-endodermal stage contributed through metabolic support in rescue from ALF in this mouse model [46]. By contrast, transplantation of HeLa cells (human cervical cancer cell line) without hepatic functions was insufficient for rescue in ALF. On the other hand, transplanted healthy liver tissue or hepatocytes release paracrine factors from ectopic locations into systemic circulation that further promote hepatic regeneration in ALF [32, 44]. However, paracrine factors may be insufficient for rescue in ALF by themselves without simultaneous hepatic support, as indicated by studies of conditioned medium from healthy hepatocytes in this NOD/SCID mouse model [32]. Therefore, secretion of beneficial paracrine factors by eFHLC, including those deficient in people with ALF, e.g., VEGF, PDGF, GCSF [41, 42], and lessening of hepatic injury in mice with ALF was in agreement with their combined replacement of hepatic functions and such hepatotrophic cytokines. Whether metabolomics products from transplanted eFHLC advanced liver regeneration in ALF is unknown.

As uniform populations of hepatocytes were generated by hTERT-FH-CM and CPs without transgenic manipulations, this will be valuable for therapies. Differentiating PSC by CPs without animal materials or feeders will provide other gains. The absence of residual undifferentiated PSC in ensuing cell populations should be reassuring in terms of oncogenetic concerns.

Supplementary Material

Refer to Web version on PubMed Central for supplementary material.

Acknowledgements

Bruce Cooper at Purdue University Metabolite Profiling Facility performed MS analysis.

Funding

Supported in part by NIH grants [R01 DK071111, R01 DK088561, P30 DK41296 and P30 CA13330] and NYSTEM [Contract Number C024172; Shared Facilities]

Abbreviations

AAT	α -1-antitrypsin
AFP	α -fetoprotein
AH	adult hepatocyte
ALB	albumin
ALF	acute liver failure
ASGPR	asialoglycoprotein receptor
ATF	cyclic AMP-dependent transcription factor
ATM	ataxia telangiectasis mutated

CCNC	cyclin C
CCND	cyclin D
CEBP	CCAAT/enhancer-binding protein
CK	cytokeratin
CM	conditioned medium
CP	metabolomic chemical product
CYP	cytochrome P450
eFHLc	early-stage fetal hepatocyte-like cells
ECAD	epithelial-cadherin
EGR	early growth response gene
ELD	expression level dominance
EM	electron microscopy
EpCAM	epithelial cell adhesion molecule
FH	fetal hepatocyte
FOXA2	forkhead box A (HNF3 beta)
FOXA3	forkhead box A (HNF3 gamma)
FXR	farnesoid X receptor
GATA:	GATA-binding protein
GDF	growth differentiation factor
G6P	glucose-6-phosphatase
GGT	gamma-glutamyltranspeptidase
GCSF	granulocyte colony-stimulating factor
H2AX	H2A histone family member X
hESC	human embryonic stem cells
hiPSC	human induced pluripotent stem cells
HNF	hepatocyte nuclear factor
ILK	integrin-linked protein kinase
IPA	Ingenuity pathway analysis
Ki67	proliferation-related Ki-67 antigen

LXR	liver x receptor
MAPK	mitogen associated protein kinase
MCT	monocrotaline
miRNA	microRNA
MSC	mesenchymal stem cells
NANOG	Nanog homeobox
NF-κB	nuclear factor kappa beta
NOTCH	notch homolog 1, translocation-associated
OCT	octamer-binding transcription factor
PDGF	platelet-derived growth factor
PDX1	pancreatic and duodenal homeobox 1
PGE2	prostaglandin E2
Phen	phenytoin
PROX	prospero homeobox 1
PSC	pluripotent stem cells
qRT-PCR	quantitative reverse-transcription polymerase chain reaction
RELA	RELA protooncogene, NF- κ B subunit
Rif	rifampicin
RXR	retinoic acid receptor
SMA	smooth muscle actin
SOX	sex determining region Y-box
TAC	Affymetrix Transcription Analysis Console, version 4
TF	transcription factor
TGF	transforming growth factor
TNF	tumor necrosis factor
TR	transcriptional regulator
TRA	sex determining transforming protein
TTR	transthyretin
TWIST	Twist family BHLH transcription factor

VEGF	vascular endothelial growth factor
VIM	vimentin
WNT	wingless integration site Nusse and Varmus

References

- [1]. Chinzei R, Tanaka Y, Shimizu-Saito K, Hara Y, Kakinuma S, Watanabe M, Teramoto K, Arai S, Takase K, Sato C, Terada N, Teraoka H Embryoid-body cells derived from a mouse embryonic stem cell line show differentiation into functional hepatocytes. *Hepatology* 2002;36:22–29. [PubMed: 12085345]
- [2]. Rambhatla L, Chiu CP, Kundu P, Peng Y, Carpenter MK. Generation of hepatocyte-like cells from human embryonic stem cells. *Cell Transplant* 2003;12:1–11. [PubMed: 12693659]
- [3]. Lavon N, Yanuka O, Benvenisty N. Differentiation and isolation of hepatic-like cells from human embryonic stem cells. *Differentiation* 2004;72:230–238. [PubMed: 15270779]
- [4]. Hay DC, Fletcher J, Payne C, Terrace JD, Gallagher RC, Snoeys J, et al. Highly efficient differentiation of hESCs to functional hepatic endoderm requires ActivinA and Wnt3a signaling. *Proc Natl Acad Sci U S A* 2008;105:12301–12306. [PubMed: 18719101]
- [5]. Shiraki N, Umeda K, Sakashita N, Takeya M, Kume K, Kume S. Differentiation of mouse and human embryonic stem cells into hepatic lineages. *Genes Cells* 2008;13:731–746. [PubMed: 18513331]
- [6]. Moore RN, Moghe PV. Expedited growth factor-mediated specification of human embryonic stem cells toward the hepatic lineage. *Stem Cell Res* 2009.
- [7]. Johannesson M, Stahlberg A, Ameri J, Sand FW, Norrman K, Semb H. FGF4 and retinoic acid direct differentiation of hESCs into PDX1-expressing foregut endoderm in a time- and concentration-dependent manner. *PLoS ONE* 2009;4:e4794. [PubMed: 19277121]
- [8]. Soto-Gutierrez A, Navarro-Alvarez N, Zhao D, Rivas-Carrillo JD, Lebkowski J, Tanaka N, et al. Differentiation of mouse embryonic stem cells to hepatocyte-like cells by co-culture with human liver nonparenchymal cell lines. *Nat Protoc* 2007;2:347–356. [PubMed: 17406596]
- [9]. Haridass D, Yuan Q, Becker PD, Cantz T, Iken M, Rothe M, et al. Repopulation efficiencies of adult hepatocytes, fetal liver progenitor cells, and embryonic stem cell-derived hepatic cells in albumin-promoter-enhancer urokinase-type plasminogen activator mice. *Am J Pathol* 2009;175:1483–1492. [PubMed: 19717639]
- [10]. Karp JM, Ferreira LS, Khademhosseini A, Kwon AH, Yeh J, Langer RS. Cultivation of human embryonic stem cells without the embryoid body step enhances osteogenesis in vitro. *Stem Cells* 2006;24:835–843. [PubMed: 16253980]
- [11]. Cai J, Zhao Y, Liu Y, Ye F, Song Z, Qin H, et al. Directed differentiation of human embryonic stem cells into functional hepatic cells. *Hepatology* 2007;45:1229–1239. [PubMed: 17464996]
- [12]. Zaret KS. Genetic programming of liver and pancreas progenitors: lessons for stem-cell differentiation. *Nat Rev Genet* 2008 9:329–340. [PubMed: 18398419]
- [13]. Freedman DA, Kashima Y, Zaret KS. Endothelial cell promotion of early liver and pancreas development. *Novartis Foundation symposium* 2007;283:207–216; discussion 216–209, 238–241. [PubMed: 18300424]
- [14]. Zalzman M, Gupta S, Giri RK, Berkovich I, Sappal BS, Karnieli O, et al. Reversal of hyperglycemia in mice by using human expandable insulin-producing cells differentiated from fetal liver progenitor cells. *Proc Natl Acad Sci U S A* 2003;100:7253–7258. [PubMed: 12756298]
- [15]. Huang P, Zhang L, Gao Y, He Z, Yao D, Wu Z, et al. Direct reprogramming of human fibroblasts to functional and expandable hepatocytes. *Cell Stem Cell* 2014;14:370–384. [PubMed: 24582927]
- [16]. Du Y, Wang J, Jia J, Song N, Xiang C, Xu J, et al. Human hepatocytes with drug metabolic function induced from fibroblasts by lineage reprogramming. *Cell Stem Cell* 2014;14:394–403. [PubMed: 24582926]

- [17]. Ang LT, Tan AKY, Autio MI, Goh SH, Choo SH, Lee KL, et al. A Roadmap for Human Liver Differentiation from Pluripotent Stem Cells. *Cell reports* 2018;22:2190–2205. [PubMed: 29466743]
- [18]. Lim KT, Lee SC, Gao Y, Kim KP, Song G, An SY, et al. Small Molecules Facilitate Single Factor-Mediated Hepatic Reprogramming. *Cell reports* 2016;15:814–829. [PubMed: 27149847]
- [19]. Yanes O, Clark J, Wong DM, Patti GJ, Sanchez-Ruiz A, Benton HP, et al. Metabolic oxidation regulates embryonic stem cell differentiation. *Nature chemical biology* 2010;6:411–417. [PubMed: 20436487]
- [20]. Marsboom G, Zhang GF, Pohl-Avila N, Zhang Y, Yuan Y, Kang H, et al. Glutamine Metabolism Regulates the Pluripotency Transcription Factor OCT4. *Cell reports* 2016;16:323–332. [PubMed: 27346346]
- [21]. Sampaziotis F dBM, Geti I, Bertero A, Hannan NR, Vallier L Directed differentiation of human induced pluripotent stem cells into functional cholangiocyte-like cells. *Nat Protoc* 2017;8:814–827. [PubMed: 28333915]
- [22]. Raju R CD, Cho DS, Park Y, Verfaillie CM, Hu WS. Cell Expansion During Directed Differentiation of Stem Cells Toward the Hepatic Lineage. *Stem Cells Dev* 2017;26:274–284. . [PubMed: 27806669]
- [23]. Fisher JB PK, Rao S, Duncan SA. GATA6 is essential for endoderm formation from human pluripotent stem cells. *Biol Open* 2017;6:1084–1095. [PubMed: 28606935]
- [24]. Malhi H, Irani AN, Gagandeep S, Gupta S. Isolation of human progenitor liver epithelial cells with extensive replication capacity and differentiation into mature hepatocytes. *J Cell Sci* 2002;115:2679–2688. [PubMed: 12077359]
- [25]. Inada M, Follenzi A, Cheng K, Surana M, Joseph B, Benten D, et al. Phenotype reversion in fetal human liver epithelial cells identifies the role of an intermediate meso-endodermal stage before hepatic maturation. *J Cell Sci* 2008;121:1002–1013. [PubMed: 18319302]
- [26]. Inada M, Benten D, Cheng K, Joseph B, Berishvili E, Badve S, et al. Stage-specific regulation of adhesion molecule expression segregates epithelial stem/progenitor cells in fetal and adult human livers. *Hepatology international* 2008;2:50–62. [PubMed: 19669279]
- [27]. Rogler CE, Bebawee R, Matarlo J, Locker J, Pattamanuch N, Gupta S, et al. Triple Staining Including FOXA2 Identifies Stem Cell Lineages Undergoing Hepatic and Biliary Differentiation in Cirrhotic Human Liver. *The journal of histochemistry and cytochemistry : official journal of the Histochemistry Society* 2017;65:33–46. [PubMed: 27879410]
- [28]. Bandi S, Gupta S, Tchaikovskaya T, Gupta S. Differentiation in stem/progenitor cells along fetal or adult hepatic stages requires transcriptional regulators independently of oscillations in microRNA expression. *Exp Cell Res* 2018;370:1–12. [PubMed: 29883712]
- [29]. Cheishvili D, Christiansen S, Stochinsky R, Pepin AS, Sapozhnikov DM, Zhou R, et al. DNA methylation controls unmethylated transcription start sites in the genome in trans. *Epigenomics* 2017;9:611–633. [PubMed: 28470094]
- [30]. Qiu C, Hanson E, Olivier E, Inada M, Kaufman DS, Gupta S, et al. Differentiation of human embryonic stem cells into hematopoietic cells by coculture with human fetal liver cells recapitulates the globin switch that occurs early in development. *Experimental hematology* 2005;33:1450–1458. [PubMed: 16338487]
- [31]. Wege H, Le HT, Chui MS, Liu L, Wu J, Giri R, et al. Telomerase reconstitution immortalizes human fetal hepatocytes without disrupting their differentiation potential. *Gastroenterology* 2003;124:432–444. [PubMed: 12557149]
- [32]. Bandi S, Joseph B, Berishvili E, Singhanian R, Wu YM, Cheng K, et al. Perturbations in ataxia telangiectasia mutant signaling pathways after drug-induced acute liver failure and their reversal during rescue of animals by cell therapy. *Am J Pathol* 2011;178:161–174. [PubMed: 21224054]
- [33]. Enami Y, Bandi S, Kapoor S, Krohn N, Joseph B, Gupta S. Hepatic stellate cells promote hepatocyte engraftment in rat liver after prostaglandin-endoperoxide synthase inhibition. *Gastroenterology* 2009;136:2356–2364. [PubMed: 19303017]
- [34]. Cho JJ, Joseph B, Sappal BS, Giri RK, Wang R, Ludlow JW, et al. Analysis of the functional integrity of cryopreserved human liver cells including xenografting in immunodeficient mice to address suitability for clinical applications. *Liver Int* 2004;24:361–370. [PubMed: 15287860]

- [35]. Gupta S, Rajvanshi P, Sokhi RP, Vaidya S, Irani AN, Gorla GR. Position-specific gene expression in the liver lobule is directed by the microenvironment and not by the previous cell differentiation state. *J Biol Chem* 1999;274:2157–2165. [PubMed: 9890978]
- [36]. Barrett T, Wilhite SE, Ledoux P, Evangelista C, Kim IF, Tomashevsky M, et al. NCBI GEO: archive for functional genomics data sets--update. *Nucleic Acids Res* 2013;41:D991–995. [PubMed: 23193258]
- [37]. Bandi S, Joseph B, Cheng K, Gupta S Spontaneous origin from human embryonic stem cells of early developmental stage liver cells displaying conjoint meso-endodermal phenotype with hepatic functions. *J Cell Sci* 2012;125:1274–1283. [PubMed: 22349702]
- [38]. Benten D, Cheng K, Gupta S. Identification of transplanted human cells in animal tissues. *Methods in molecular biology (Clifton, NJ)* 2006;326:189–201.
- [39]. Babicki S, Arndt D, Marcu A, Liang Y, Grant JR, Maciejewski A, et al. Heatmapper: web-enabled heat mapping for all. *Nucleic acids research* 2016;44:W147–153. [PubMed: 27190236]
- [40]. Lee WM. Acetaminophen (APAP) hepatotoxicity-Isn't it time for APAP to go away? *J Hepatol* 2017;S0168-8278:32148–32147.
- [41]. Steuerwald NM, Foureau DM, Norton HJ, Zhou J, Parsons JC, Chalasani N, et al. Profiles of serum cytokines in acute drug-induced liver injury and their prognostic significance. *PLoS One* 2013;8:e81974. [PubMed: 24386086]
- [42]. Takayama H, Miyake Y, Nouse K, Ikeda F, Shiraha H, Takaki A, et al. Serum levels of platelet-derived growth factor-BB and vascular endothelial growth factor as prognostic factors for patients with fulminant hepatic failure. *Journal of gastroenterology and hepatology* 2011;26:116–121.
- [43]. Bird TG, Muller M, Boulter L, Vincent DF, Ridgway RA, Lopez-Guadamillas E, et al. TGFbeta inhibition restores a regenerative response in acute liver injury by suppressing paracrine senescence. *Science translational medicine* 2018;10.
- [44]. Kakabadze Z, Kakabadze A, Chakhunashvili D, Karalashvili L, Berishvili E, Sharma Y, et al. Decellularized human placenta supports hepatic tissue and allows rescue in acute liver failure. *Hepatology* 2018;67:1956–1969. [PubMed: 29211918]
- [45]. Cheng K, Benten D, Bhargava K, Inada M, Joseph B, Palestro C, et al. Hepatic targeting and biodistribution of human fetal liver stem/progenitor cells and adult hepatocytes in mice. *Hepatology* 2009;50:1194–1203. [PubMed: 19637284]
- [46]. Bandi S, Cheng K, Joseph B, Gupta S. Spontaneous origin from human embryonic stem cells of liver cells displaying conjoint meso-endodermal phenotype with hepatic functions. *J Cell Sci* 2012;125:1274–1283. [PubMed: 22349702]
- [47]. Mirzahassemi A, Noszal B. Species-Specific Standard Redox Potential of Thiol-Disulfide Systems: A Key Parameter to Develop Agents against Oxidative Stress. *Sci Rep* 2016;6:37596. [PubMed: 27869189]
- [48]. Viswanathan P, Sharma Y, Gupta P, Gupta S. Replicative stress and alterations in cell cycle checkpoint controls following acetaminophen hepatotoxicity restrict liver regeneration. *Cell Prolif* 2018;51:e12445. [PubMed: 29504225]
- [49]. Echeverri-Ruiz N, Haynes T, Landers J, Woods J, Gemma MJ, Hughes M, et al. A biochemical basis for induction of retina regeneration by antioxidants. *Developmental biology* 2018;433:394–403. [PubMed: 29291983]
- [50]. Chung JH, Kim YS, Noh K, Lee YM, Chang SW, Kim EC. Deferoxamine promotes osteoblastic differentiation in human periodontal ligament cells via the nuclear factor erythroid 2-related factor-mediated antioxidant signaling pathway. *Journal of periodontal research* 2014;49:563–573. [PubMed: 24111577]
- [51]. Ardite E, Barbera JA, Roca J, Fernandez-Checa JC. Glutathione depletion impairs myogenic differentiation of murine skeletal muscle C2C12 cells through sustained NF-kappaB activation. *Am J Pathol* 2004;165:719–728. [PubMed: 15331397]
- [52]. Park JH, Lee JM, Lee EJ, Kim DJ, Hwang WB. Kynurenine promotes the goblet cell differentiation of HT-29 colon carcinoma cells by modulating Wnt, Notch and AhR signals. *Oncol Rep* 2018;39:1930–1938. [PubMed: 29436668]

- [53]. Vidal C1 LW, Santner-Nanan B, Lim CK, Guillemin GJ, Ball HJ, Hunt NH, Nanan R, Duque G. The kynurenine pathway of tryptophan degradation is activated during osteoblastogenesis. *Stem Cells* 2015;1:111–121.
- [54]. Rodgers A, Mormeneo D, Long JS, Delgado A, Pyne NJ, Pyne S. Sphingosine 1-phosphate regulation of extracellular signal-regulated kinase-1/2 in embryonic stem cells. *Stem cells and development* 2009;18:1319–1330. [PubMed: 19228106]
- [55]. Sigruener A, Tarabin V, Paragh G, Liebisch G, Koehler T, Farwick M, et al. Effects of sphingoid bases on the sphingolipidome in early keratinocyte differentiation. *Experimental dermatology* 2013;22:677–679. [PubMed: 24079743]
- [56]. Yoo DY, Kim W, Kim DW, Yoo KY, Chung JY, Youn HY, et al. Pyridoxine enhances cell proliferation and neuroblast differentiation by upregulating the GABAergic system in the mouse dentate gyrus. *Neurochemical research* 2011;36:713–721. [PubMed: 21207138]

Highlights

- Cell interactions capable of inducing stem cell differentiation are not well understood;
- In this study soluble substances from fetal hepatocytes induced stem cell differentiation;
- Differentiation-inducing substances constituted a series of metabolomic products;
- The extent of hepatic differentiation in cells was sufficient for rescue in liver failure;
- This will advance mechanisms in tissue homeostasis and regenerative medicine.

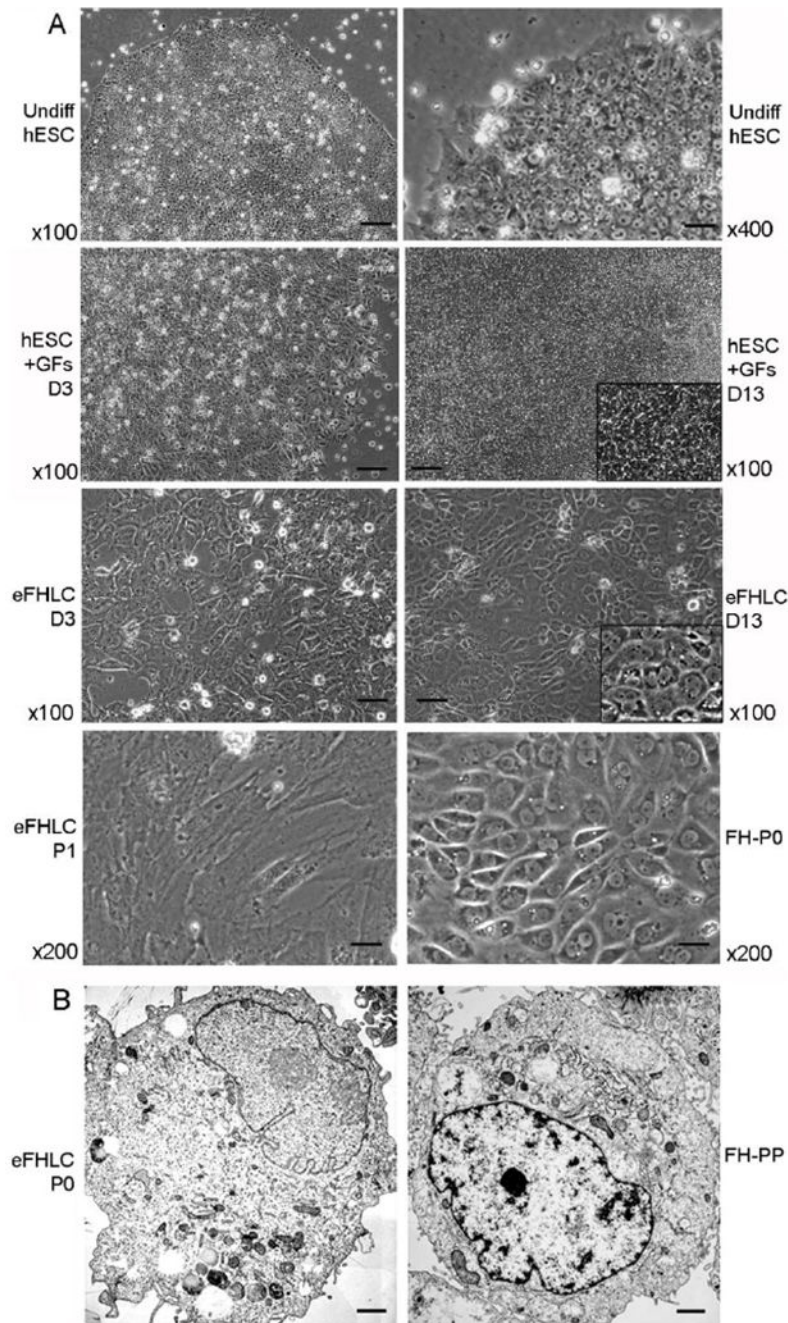


Fig. 1. hESC cultured with FHB-CM shifted to epithelial morphology resembling hepatocytes. (A) Phase contrast microscopy: Undifferentiated hESC under lower and higher magnifications as indicated (top); hESC treated with growth factors and other additives alone (GFs) after 3d and 14d (second from top); eFHLc derived from hESC cultured with hTERT-FH-CM for 3d or 14d (second from bottom); and eFHLc after first passage (P1) compared with primary fetal hepatocytes (FH) in initial culture (P0) (bottom panel). In hESC cultured with GFs, cells did not develop epithelial morphology (inset, higher magnification shows cells with morphology of hESC). By contrast, culture of hESC with

hTERT-FH-CM led to morphological alterations within 3d. By 13-14 d, these eFHLC universally exhibited epithelial morphology – inset, higher magnification including cells with binucleation – a feature of hepatocytes. Original magnification $\times 100-400$; scale bars, 15 μm . (B) Transmission EM of eFHLC and freshly-isolated fetal hepatocytes without culture (FH-PP). In these cell types, nucleus was often to the side with vesicles or microperoxisomes characteristic of hepatocytes (scale bar, 1 μm).

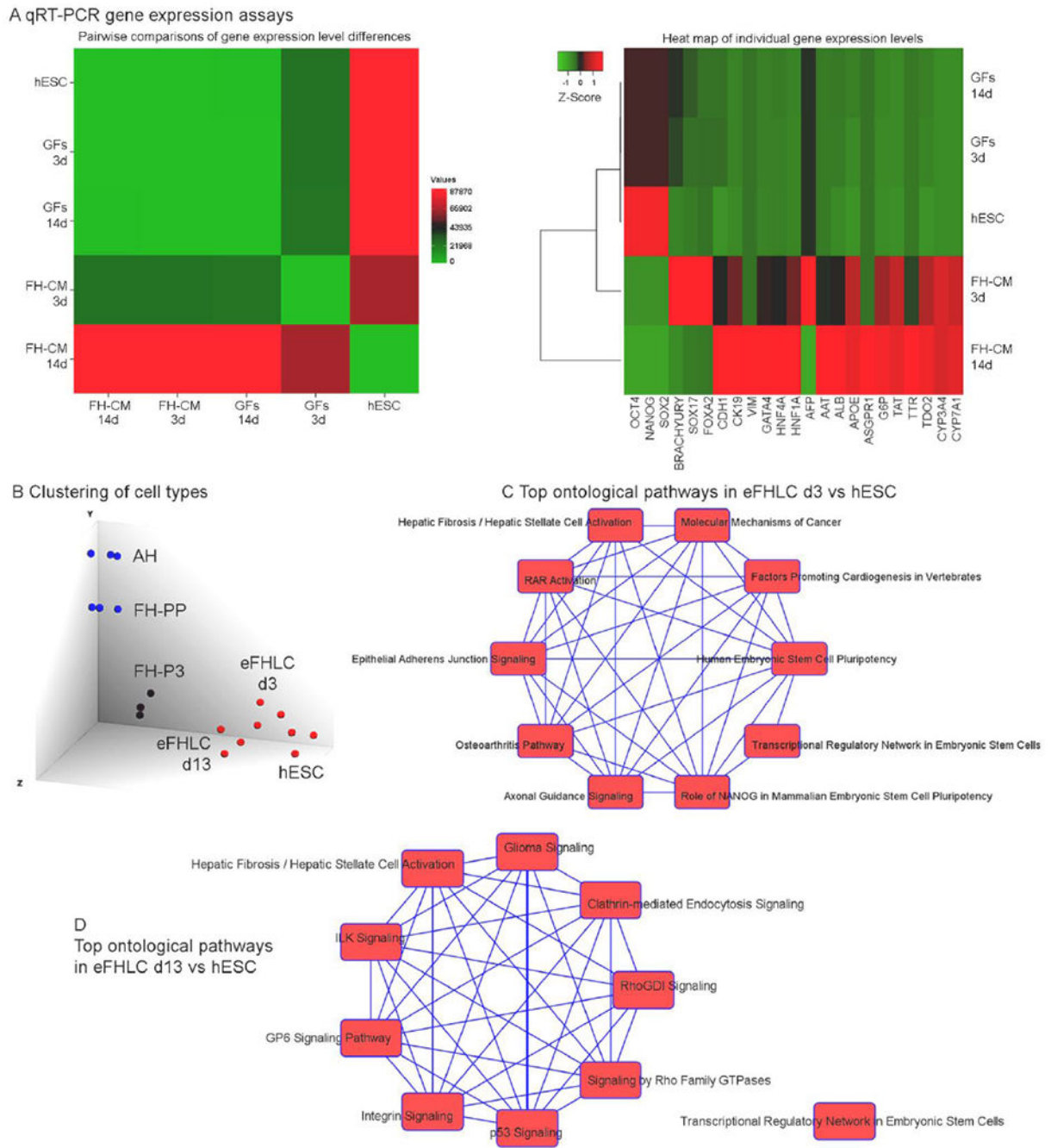


Fig. 2. Gene expression differences in hESC-derived cells with representation of hepatic foregut endoderm and various ontological pathways.

(A) Cumulative analysis of mRNA expression (n=23) by qRT-PCR in undifferentiated hESC and hESC-derived cells 3d or 14d after differentiation with either GFs alone or hTERT-FH-CM plus GFs. Pairwise comparisons indicated significantly greater gene expression level in hTERT-FH-CM condition, $p < 0.0006$, ANOVA (left). Heat map for expression of individual genes analyzed (right) indicated pluripotency markers (OCT4, NANOG and SOX2) declined much less after GFs alone compared with hTERT-FH-CM plus GFs. The gene expression pattern in respect to endoderm (SOX17, FOXA2) and mesoderm (brachyury), which

appeared transiently before hepatic TFs (GATA4, HNF4, HNF1A) after hTERT-FH-CM plus GFs was not reproduced by GFs alone. Similarly, after hTERT-FH-CM plus GFs, epithelial (CDH1), biliary (CK19), mesenchymal (VIM), and hepatic genes (ALB, AAT, ASGPR, TTR, others indicated in heat map) were expressed more than after GFs alone: Gene expression levels normalized to undifferentiated hESC after 14d in hTERT-FH-CM plus GFs or GFs alone were 82 ± 35 -fold versus 2.0 ± 0.3 -fold, respectively, $p < 0.001$. (B) Cell type clustering by mRNA profiles from Affymetrix arrays with TAC. This indicated divergence of eFHLC from hESC; these converged along FH cultured for three passages (FH-P3). In turn, FH-P3 diverged from freshly-isolated fetal (FH-PP) or adult hepatocytes (AH). (C-D) Ontological pathways (top 10) exhibited versus hESC in eFHLC cultured in hTERT-FH-CM for 3d (C) or 13d (D). These pathways shifted from the top category of hESC pluripotency after 3d to that of inflammation (hepatic fibrosis pathways), extracellular matrix (ILK signaling) and others after 13d. This verified hTERT-FH-CM exerted rapid and major effects on hESC differentiation (**complete pathway listings are in Suppl. Tables S2 and S3**).

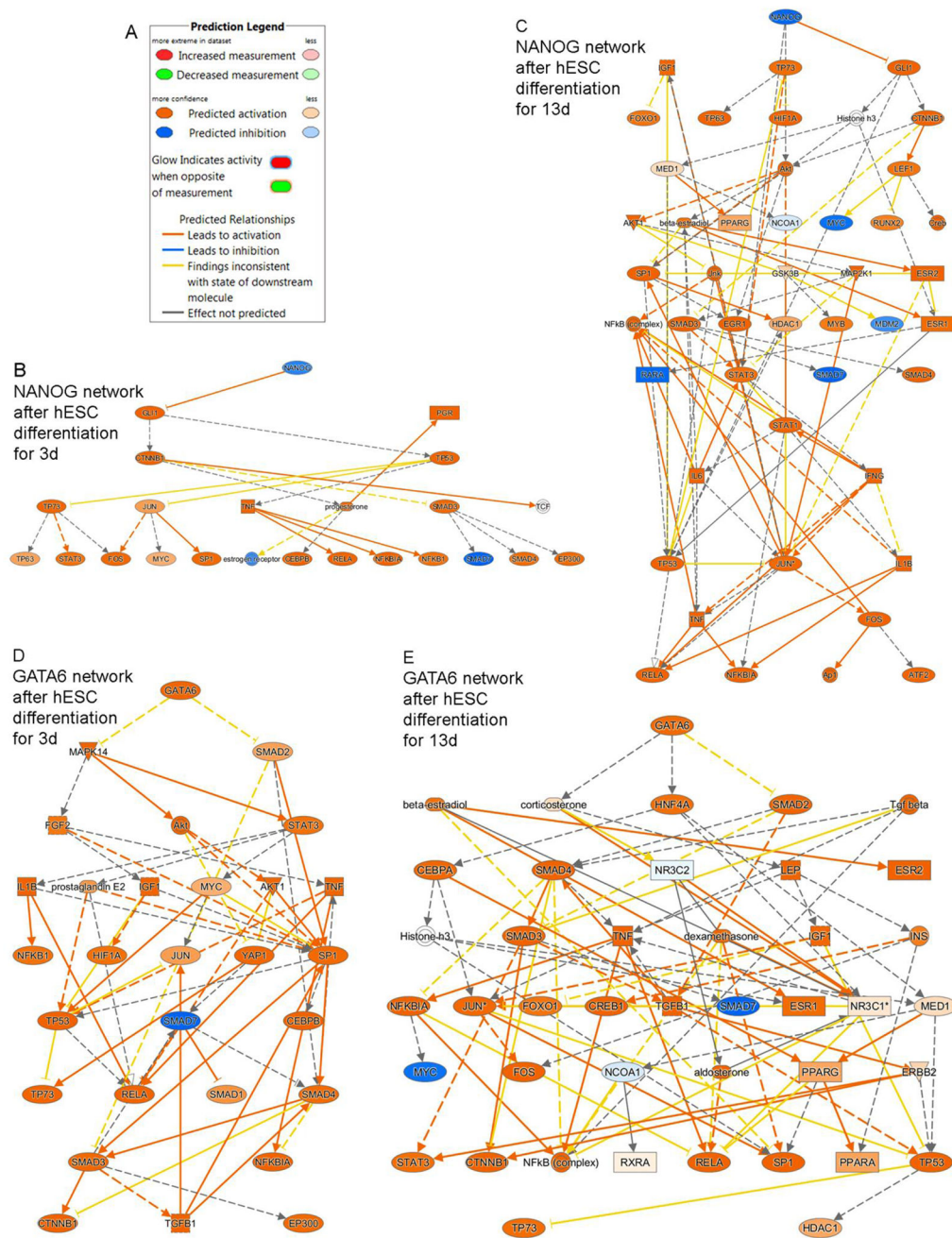


Fig. 3. Mechanistic networks identified by IPA in eFHLc versus hESC indicated inactivation of pluripotency-inducing (NANOG) and activation of differentiation-inducing (GATA6) regulators. (A) Prediction legend for network regulation. (B-C) Inactivation in eFHLc of NANOG network (blue color) took place early (d3) and continued subsequently (d13). (C-D) By contrast, GATA6 network accompanying hepatic differentiation was reciprocally activated (orange color). As cell differentiation advanced over 13d, more network nodes were included in networks. Individually, downstream members of networks additionally oversee

survival, proliferation, apoptosis, and other events. (**Additional TRs are in Suppl. Table S4**).

Author Manuscript

Author Manuscript

Author Manuscript

Author Manuscript

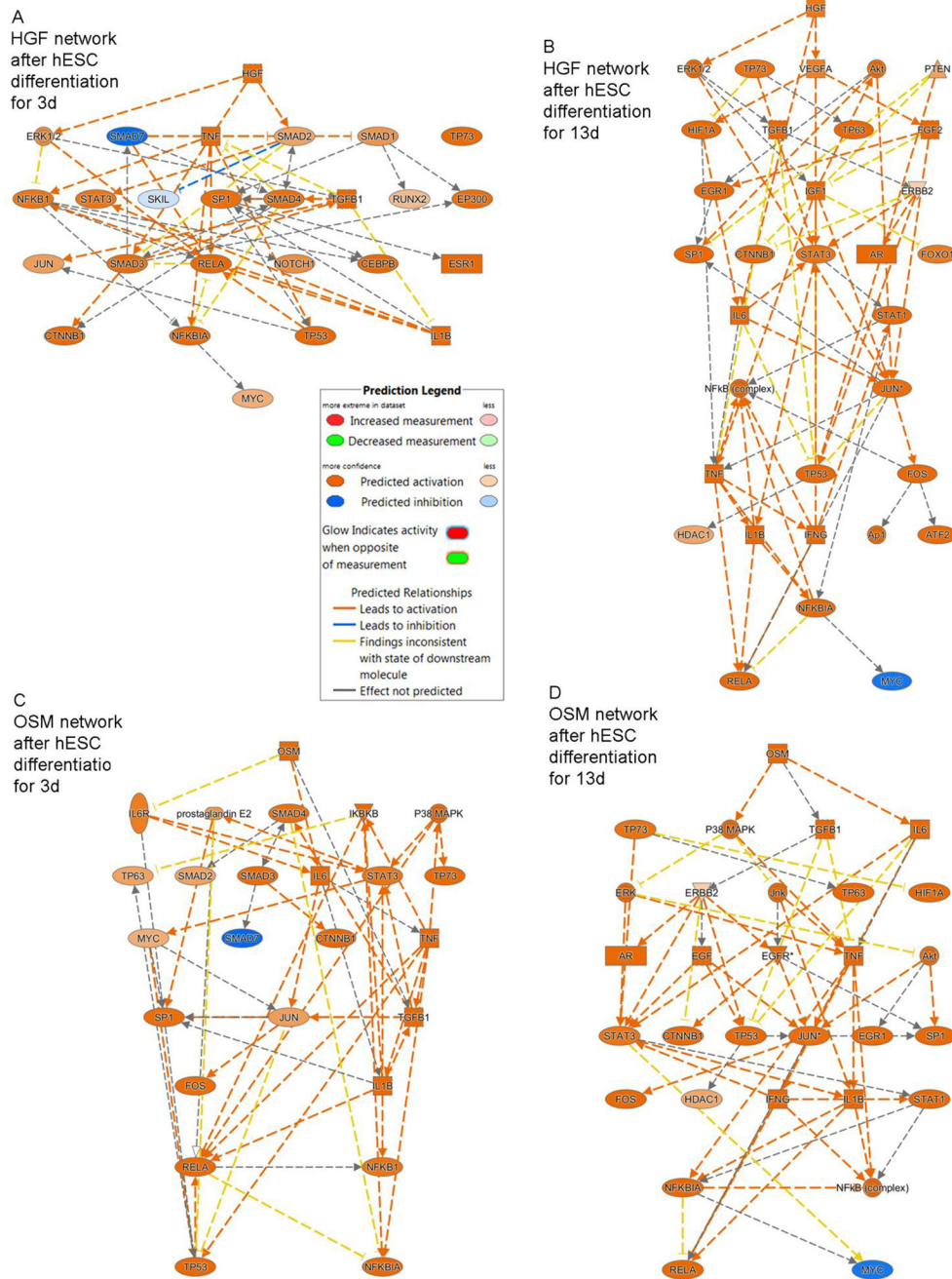


Fig. 4. Mechanistic networks identified by IPA of HGF and OSM in eFHLc versus hESC. (A, C) HGF and OSM networks were variably activated in eFHLc after 3d of culture in hTERT-FH-CM with addition of only RA. Subsequently, network profiles at d13 remained essentially similar, although more TRs were recruited during supplementation of hTERT-FH-CM with HGF, OSM and other additives (B, D). Prediction legend for network regulation is included. The TRs represented processes of cell injury (TNF, TGFb, IL6 and related signaling pathways, e.g., SMADs); inflammation (NFkB, RELA, others); cytoprotection (STAT3, AKT); or cell growth (JUN, FOS, MYC, p53). Differentiation

regulators (NOTCH1, CTNNB1 or HDAC1) were inconsequential since experimental manipulation of these pathways did not advance hepatic properties (**Additional effects of retinoic acid receptors are in Suppl. Fig. S1**).

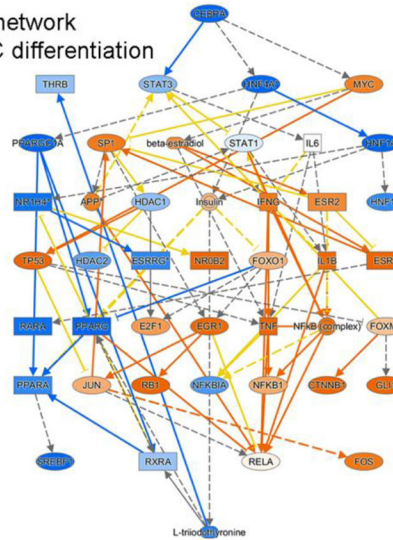
Author Manuscript

Author Manuscript

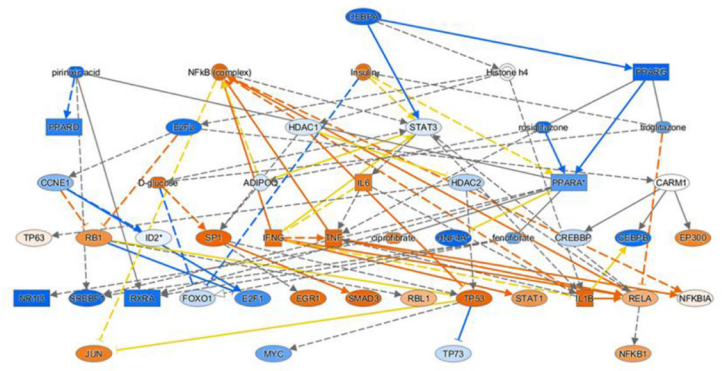
Author Manuscript

Author Manuscript

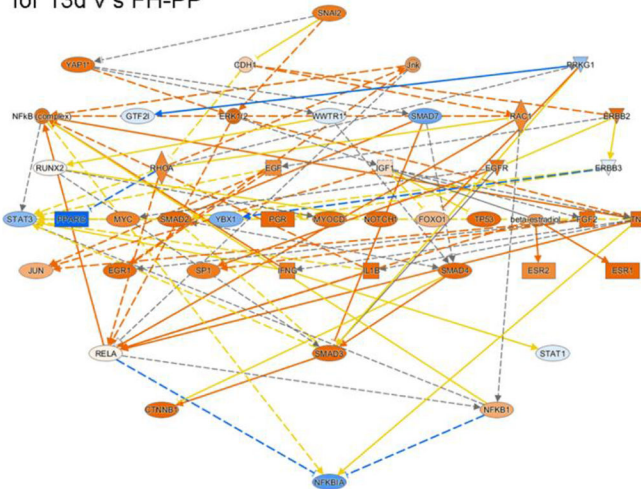
A CEBPA network after hESC differentiation for 13d vs FH-PP



B CEBPA network in FH-P3 vs FH-PP



C SNAI2 network after hESC differentiation for 13d v s FH-PP



D SNAI2 network in FH-P3 vs FH-PP

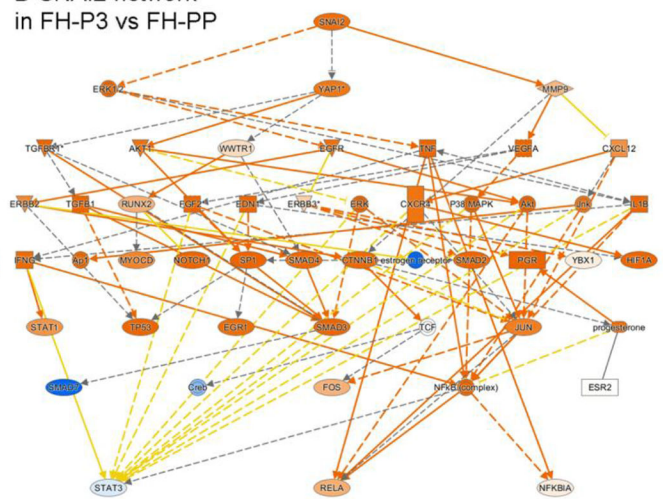


Fig. 5. Upstream networks for hepatic differentiation staging.

Mechanistic networks for CEBPA (A-B) and SNAI2 (C-D) are presented versus freshly isolated FH (FH-PP) according to IPA. The CEBPA network was less active in both eFHLC and FH-P3 (three passages in culture of FH-PP). By contrast, SNAI2 network was active in eFHLC and FH-P3. This was in agreement with hepatic plus mesenchymal gene expression. The prevalence in eFHLC and FH-PP was generally similar of less active (in blue) or more active (in orange) downstream regulators. This assigned eFHLC to early fetal-like hepatic stage. Key to prediction legends is in Fig. 3. And 4 (Suppl. Table S5 lists TRs).

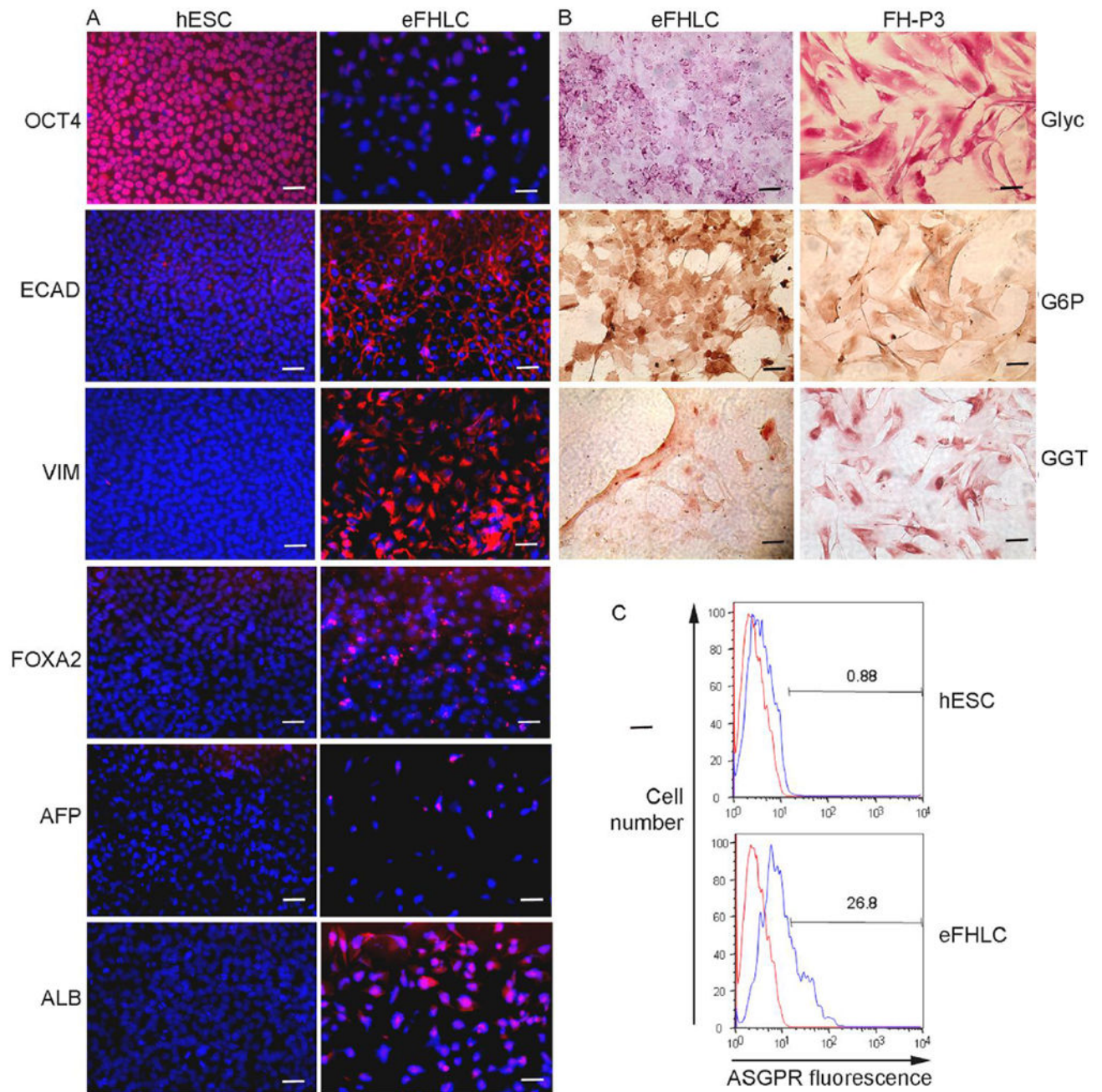


Fig. 6. Cytostainings for proteins verified early hepatic differentiation in eFHLC.

(A) Immunostaining for markers in hESC vs eFHLC. In d14 eFHLC, OCT4 was not expressed, indicating loss of pluripotency; FOXA2 was present to indicate hepatic endoderm was induced; AFP was infrequently expressed (<5%), since ALB was present (80-90%); ECAD expression in cells (100%) indicated their epithelial nature; while simultaneous VIM expression (80-90%) indicated mesenchymal property. (B) Histochemical staining of eFHLC and FH-P3 indicated these cells simultaneously expressed hepatobiliary markers (glycogen, G6P and GGT in 100%). Original magnifications, x400; scale bars 15 μ m. (C) Flow

cytometry for asialoglycoprotein receptor (ASGPR) indicated 27% eFHLC expressed this characteristic hepatic marker. This was in agreement with representation of eFHLC along fetal-like hepatic stage.

Author Manuscript

Author Manuscript

Author Manuscript

Author Manuscript

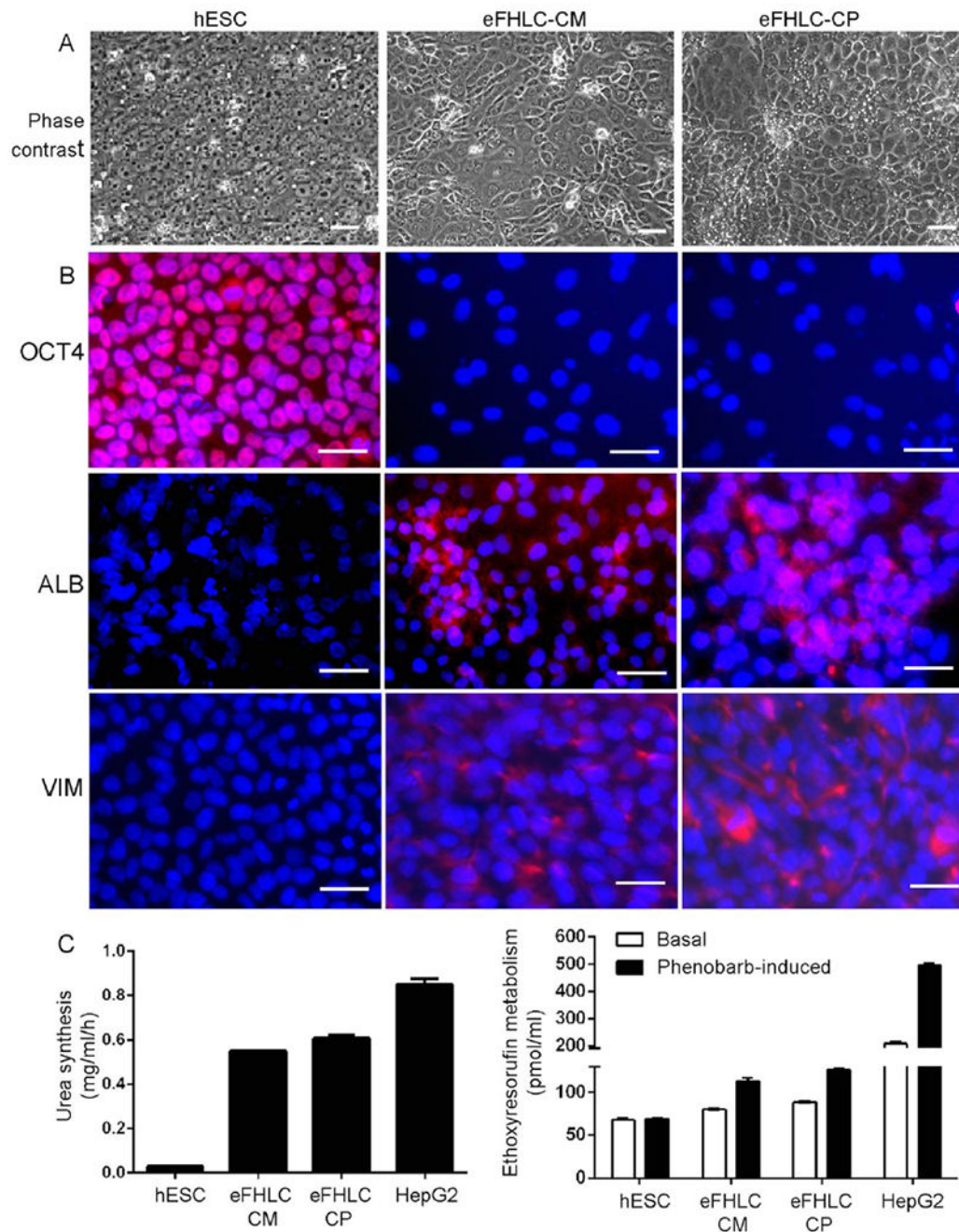


Fig. 7. Metabolomics products generated eFHLC from hESC.

(A) Undifferentiated hESC (panels on left), hESC cultured with hTERT-FH-CM (middle) and hESC cultured with combination of seven CPs (right). Phase contrast microscopy showing epithelial morphology in hESC cultured with either hTERT-FH-CM or 10 μ m amounts of CPs. Original magnifications, $\times 200$; scale bars 15 μ m. (B) Immunofluorescence staining for markers. This indicated loss of OCT4 and gain of ALB or VIM (red color) in eFHLC generated by hTERT-FH-CM or CPs. Nuclei are stained with DAPI. Original magnifications, $\times 400$; scale bars 15 μ m. (C) Metabolic functions in eFHLC from either

hTERT-FH-CM or CPs with albumin and urea synthesis and conversion of ethoxyresorufin to resorufin. Differences in eFHLC from undifferentiated hESC were significant; although HepG2 cells were metabolically more active, $p < 0.05$, ANOVA. (Suppl. Fig. S5 **for hiPSC differentiation**; Suppl. Table S6 **for list of CPs**; Suppl. Table S7 **for effects of CPs**).

Author Manuscript

Author Manuscript

Author Manuscript

Author Manuscript

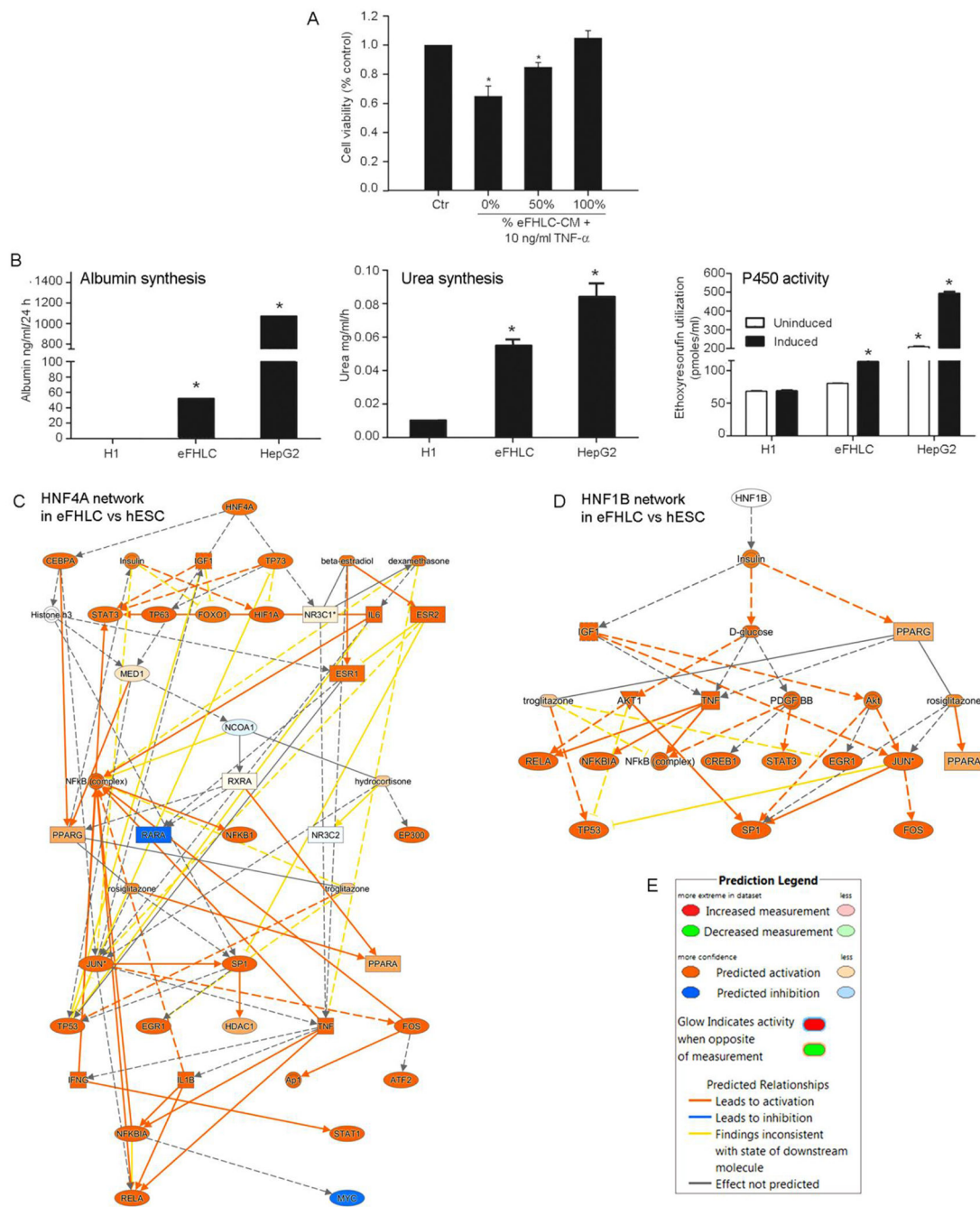


Fig. 8. Hepatic functions and cytoprotective effects in eFHLC.

(A) TNF- α cytotoxicity assay using primary mouse hepatocytes for protection from cytokines secreted by eFHLC. (Secreted cytokines in eFHLC-CM are in Suppl. Fig. S6). (B) Albumin or urea synthesis and ethoxyresorufin conversion. These concerned undifferentiated hESC, eFHLC after differentiation for 14d and HepG2 human hepatocyte cell line. Asterisks indicate $p < 0.05$ versus TNF-untreated controls (A) or undifferentiated hESC (B). (C-D) Mechanistic networks are shown for HNF4A and HNF1B in eFHLC versus undifferentiated hESC. These TRs regulate hepatic gene expression through

numerous targets. The network nodes are noteworthy for multiple additional processes related to cell differentiation, proliferation and other mechanisms. (E) Network prediction legend.

Author Manuscript

Author Manuscript

Author Manuscript

Author Manuscript

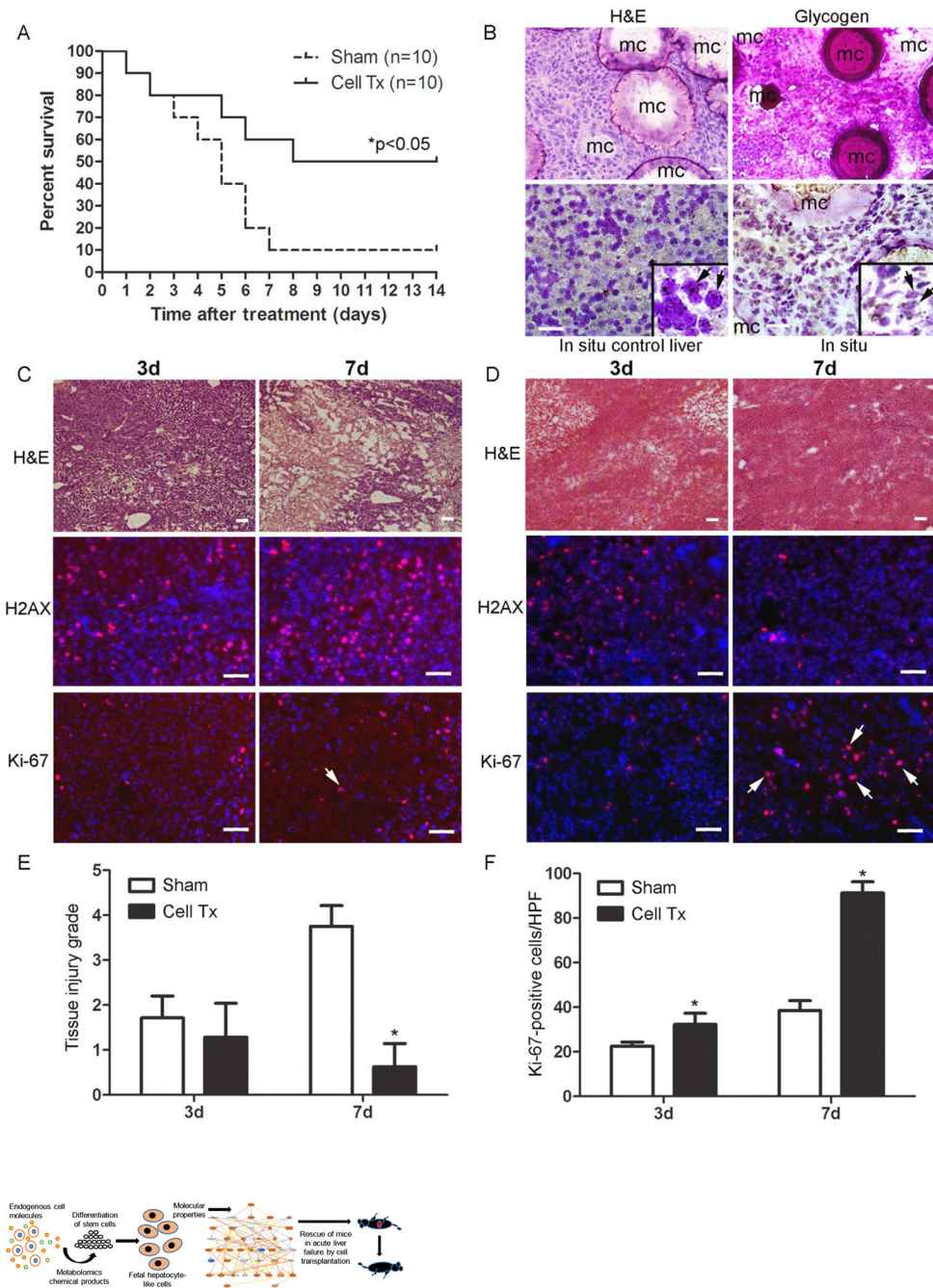


Fig. 9. Transplantation of eFHLC in mice with ALF.

(A) Survival curves indicating lowering of mortality by transplanted eFHLC. (B) Histological sections of microcarriers (mc) and transplanted cells after 7d with vascular reorganization (H&E staining), glycogen (red color in cytoplasm) and primate-specific centromeres (dark spots over nuclei; arrows in insets), in control human liver - panel on left - or transplanted cells (C-D). Liver necrosis, DNA double-strand breaks and hepatocyte proliferation in tissue sections by H&E, γ H2AX, and Ki67 staining, respectively, in mice with vehicle alone (C) or eFHLC (D). (E-F) Tissue injury grading (E) and Ki67+

proliferating cells in liver. Original magnifications, $\times 100$ -200; scale bars 15 μm . Asterisks, $p < 0.05$ (Suppl. Table S8 **for liver gene expression**).

Author Manuscript

Author Manuscript

Author Manuscript

Author Manuscript